Cardiovascular Research (2012) **96**, 73–80
doi:10.1093/cvr/cvs239

Coordination of fibronectin adhesion with contraction and relaxation in microvascular smooth muscle

Zhongkui Hong[1], Zhe Sun[1], Zhaohui Li[1], Walatta-Tseyon Mesquitta[1†], Jerome P. Trzeciakowski[2], and Gerald A. Meininger[1,3*]

[1]Dalton Cardiovascular Research Center, University of Missouri, 134 Research Park Dr., Columbia, MO 65211, USA; [2]Department of Systems Biology, Texas A&M University, College Station, TX, USA; and [3]Department of Pharmacology and Physiology, University of Missouri, Columbia, MO, USA

Received 3 April 2012; revised 29 June 2012; accepted 11 July 2012; online publish-ahead-of-print 16 July 2012

Time for primary review: 40 days

Aims The regulation of vascular diameter by vasoconstrictors and vasodilators requires that vascular smooth muscle cells (VSMCs) be physically coupled to extracellular matrix (ECM) and neighbouring cells in order for a vessel to mechanically function and transfer force. The hypothesis was tested that integrin-mediated adhesion to the ECM is dynamically up-regulated in VSMCs during contractile activation in response to a vasoconstrictor and likewise down-regulated during relaxation in response to a vasodilator.

Methods and results VSMCs were isolated from the Sprague-Dawley rat cremaster muscles. Atomic force microscopy (AFM) with fibronectin (FN)-functionalized probes was employed to investigate the biomechanical responses and adhesion of VSMCs. Responses to angiotensin II (Ang II; 10^{-6} M) and adenosine (Ado; 10^{-4} M) were recorded by measurements of cell cortical elasticity and cell adhesion. The results showed that Ang II caused an immediate increase in adhesion (+27%) between the probe and cell. Cell stiffness increased (+70%) in parallel with the adhesion change. Ado decreased adhesion (−15%) to FN and reduced (−30%) stiffness.

Conclusion Changes in the receptor-mediated activation of the contractile apparatus cause parallel alterations in cell adhesion and cell cortical elasticity. These studies support the hypothesis that the regulation of cell adhesion is coordinated with contraction and demonstrate the dynamic nature of cell adhesion to the ECM. It is proposed that coordination of adhesion and VSMC contraction is an important mechanism that allows for an efficient transfer of force between the contractile apparatus of the cell and the extracellular environment.

Keywords Vascular smooth muscle cell • Vascular control • Cell adhesion • Cell elasticity • AFM

1. Introduction

The mechanical function of vascular smooth muscle cells (VSMCs) is anchorage dependent and requires the physical association of cells with the extracellular matrix (ECM) and neighbouring cells to perform the force-transfer functions associated with regulating vascular diameter.[1,2] Integrin-mediated adhesion of VSMCs to ECM proteins provides an important physical connection between the ECM and cytoskeleton for bi-directionally transmitting mechanical forces and the generation of biochemical cell signals through inside-out and outside-in mechanisms.[3–6] Importantly, we have previously demonstrated that integrins are linked to the regulation of arteriolar diameter[7,8] and the vascular myogenic response.[9] Also, a series of recent studies from tracheal and VSMCs have indicated that contraction is accompanied by parallel remodelling of both contractile and non-contractile components of the actin cytoskeleton and adhesion junctions.[2,10,11] Whether these events are coupled to changes in integrin adhesion has not been demonstrated. Also, it remains to be elucidated that whether the contraction and/or relaxation of VSMCs is actually temporally synchronized with changes in integrin adhesion in a manner that would allow it to rapidly adapt to altered mechanical loads.

Atomic force microscopy (AFM) has been used as a powerful investigative tool for work at the macro-scale live cell[12] and tissues and at

† Present address. School of Medicine and Public Health, University of Wisconsin, 1300 University Ave, B370 SMI, Madison, WI 53706, USA.

* Corresponding author. Tel: +1 573 882 9662; fax: +1 573 884 4232, Email: meiningerg@missouri.edu

the nano-scale for study of single molecules in biological research.[13,14] In addition to the imaging and topology, AFM has found many uses as related to its ability to detect and apply mechanical forces in the nano and pico newton range,[15] such as measuring the unfolding forces necessary to probe molecular structure[16,17] or unbinding forces related to cell adhesion molecules.[18–20] In this study, AFM was used for real-time monitoring of cell stiffness and adhesion that allowed us to extend analyses of these variables into the time domain to investigate their dynamic behaviour and correlate them with each other. The ability of the AFM to simultaneously assess cellular mechanical properties and adhesion make it an ideal technique to biomechanically test the hypothesis that adhesion to the ECM protein-fibronectin (FN) is dynamically regulated in VSMCs during alterations contractile activation. According to our hypothesis, integrin-mediated adhesion of VSMCs to the ECM is up-regulated during contractile activation in response to a vasoconstrictor and likewise down-regulated during relaxation in response to a vasodilator. Using AFM probes coated with FN, force curves were continuously sampled over time to permit cell stiffness to be quantified from the AFM probe approaching trace and cell adhesion to be assessed from the AFM probe retraction trace.

2. Methods

2.1 Animal model

Sprague-Dawley rats were used for this study and were maintained in accordance with guidelines for the *Guide for the Care and Use of Laboratory Animals* (NIH 83-23, revised 1996). Rats were anaesthetized by ip injection of pentobarbitol sodium (Lundbeck, Inc., Deerfield, IL, USA) at 0.1 g/kg. A surgical plane of anaesthesia was confirmed by observing no spinal reflex to a toe pinch. The rat cremaster muscle was excised via a scrotal surgical incision while animal remained under anaesthesia. Immediately after dissection, the rat was euthanized by intracardial injection of saturated KCl solution (3 ml), followed by bilateral pneumothorax. The animal facilities are approved by the Association for Assessment and Accreditation of Laboratory Animal Care (AALAC) and the animal protocol (#7416) was reviewed and approved by the Animal Care and Use Committee (ACUC) of the University of Missouri.

2.2 VSMCs isolation and culture

VSMCs were enzymatically isolated from the first-order arteriole (100–150 μm diameter) of Sprague-Dawley rat cremaster skeletal muscles using previously described methods.[21] Cells were maintained under culture conditions in DMEMF-12 supplemented with 10% foetal bovine serum (FBS, ATLANTA Biologicals, Lawrenceville, GA, USA), 10 mM 4-(2-hydroxyethyl)-1-piperazineethanesulfonic acid (HEPES, Sigma, St Louis, MO, USA), 2 mM L-glutamine, 1 mM sodium pyruvate, 100 U/mL penicillin, and 100 μg/mL streptomycin. Cells were plated on a 12 mm circular cover slip (Electron Microscopy Sciences, Hatfield, PA, USA) in a 12-well cell culture plate (Corning incorporated, Corning, NY, USA) and kept in a humidified incubator (Heraeus Instruments, Newtown, CT, USA) with 5% CO_2 at 37°C. For AFM experiments, cover slip attached cells were transferred to 60 mm tissue culture dishes (World Precision Instruments, Sarasota, FA, USA). The cells used in all experiments were maintained 3–12 days without passage. Except for HEPES and FBS, all reagents were purchased from Invitrogen (Carlsbad, CA, USA).

2.3 FN coating of AFM probes

The spherical AFM Probe (Veeco-MLCT) was functionalized with FN by the following AFM Probe decorating procedure described by Lehenkari and Horton[22] and previously used in our laboratory.[23] Briefly, Polyethylene glycol (PEG, Sigma, St Louis, MO, USA) was used as a cross-linker for FN (Invitrogen, Carlsbad, CA, USA) onto glass micro bead. The probe was first incubated with 10 mM PEG (5 min), washed with phosphate buffered saline (PBS), and then incubated with FN (0.25 mg/mL) for 5 min followed by washing in PBS. Probe spring constants were assumed to be unchanged after the labelling.

2.4 Biomechanical properties measurement with AFM

A schematic diagram of the AFM protocol is illustrated in Supplementary material online, *Figure S1*. Real-time monitoring of biomechanical properties of single mVSMCs was performed with a Bioscope AFM System (model IVa, Digital Instruments, Santa Barbara, CA, USA) that was mounted on an IX81 OLYMPUS inverted microscope (Olympus America, Inc.). The FN-decorated spherical probe with 5 μm diameter was used to repeatedly indent and retract from the cell surface at 0.1 Hz sampling frequency, 320 nm/s piezo scanning speed, and 1600 nm ramp size. For each experiment, cells (serum-starved overnight) were randomly selected and indented at a site midway between the nucleus and cell margin to collect ~60 force curves within 10 min for a pre-drug period followed by 240 force curves over 40 min for the post-drug condition. To minimize the drift, after the probe was submerged in cell bath, the whole system was thermally and mechanically equilibrated for 1 h. All of AFM measurements were conducted at room temperature in serum-free medium. The analysis of force curves was automated using a proprietary software package (NforceR).

The stiffness measured with the nano-indentation protocol is an estimate of Young's modulus of elasticity (*E*-modulus) for the cell cortex. This primarily reflects the mechanical characteristics of the submembranous cytoskeleton structure. The cell cortex contains several proteins including filamentous actin, microtubules, and intermediate filaments and has been reported to be ~600 nm in thickness and can be up to 50 nm under cell plasma membrane.[24] In this study, the indentation depth was mostly controlled ~100 nm. Over this range of indentation the stiffness measurements would thus reflect the mechanical properties of the near membrane cytoskeleton.

As shown in Supplementary material online, *Figure S2*, the cell cortex exhibits the typical viscoelastic properties, i.e. the indentation depth significantly decreased as sampling frequency was increased. Several different models have been applied to analyse the cell elasticity measured with AFM.[25–28] To date the Hertz model has been the most widely used algorithm for the characterization of live cell elasticity with AFM. It is acknowledged that this is an estimated property as the assumptions of the Hertz model are not completely satisfied since the biological properties of live cells are finite, viscoelastic, or anisotropic.[25–27] However, if live cells are indented slowly enough then these assumptions could be approximately met. Under these conditions then the viscous properties of the cell will have a limited effect on the force measurements and the elastic behaviour will dominate the cell deformation process.[29,30] Therefore, it was concluded that the Hertz model could be employed to analyse the AFM force curve to assess the VSMC elasticity. Briefly, the modified Hertz model was employed to get the following combination between the force (F) exerted by the AFM probe on the cell surface and the corresponding indentation depth (δ) of cell:[31,32]

$$F = \frac{4}{3} \cdot \frac{\sqrt{r_b E}}{1-\nu^2} \cdot \delta^{3/2}.$$

Here, E is the *E*-modulus; ν is the Poisson ratio of cell. Cells were assumed to obey elastic properties of a gel, so the Poisson ratio ν was assumed as 0.5.[31] As illustrated in Supplementary material online, *Figure S3*, the indentation depth was calculated as $\delta = z - d$, where z is the vertical travelling distance of Piezo that control the cantilever moving from the contact point (position 1) to the maximum indentation point (position 2), d is

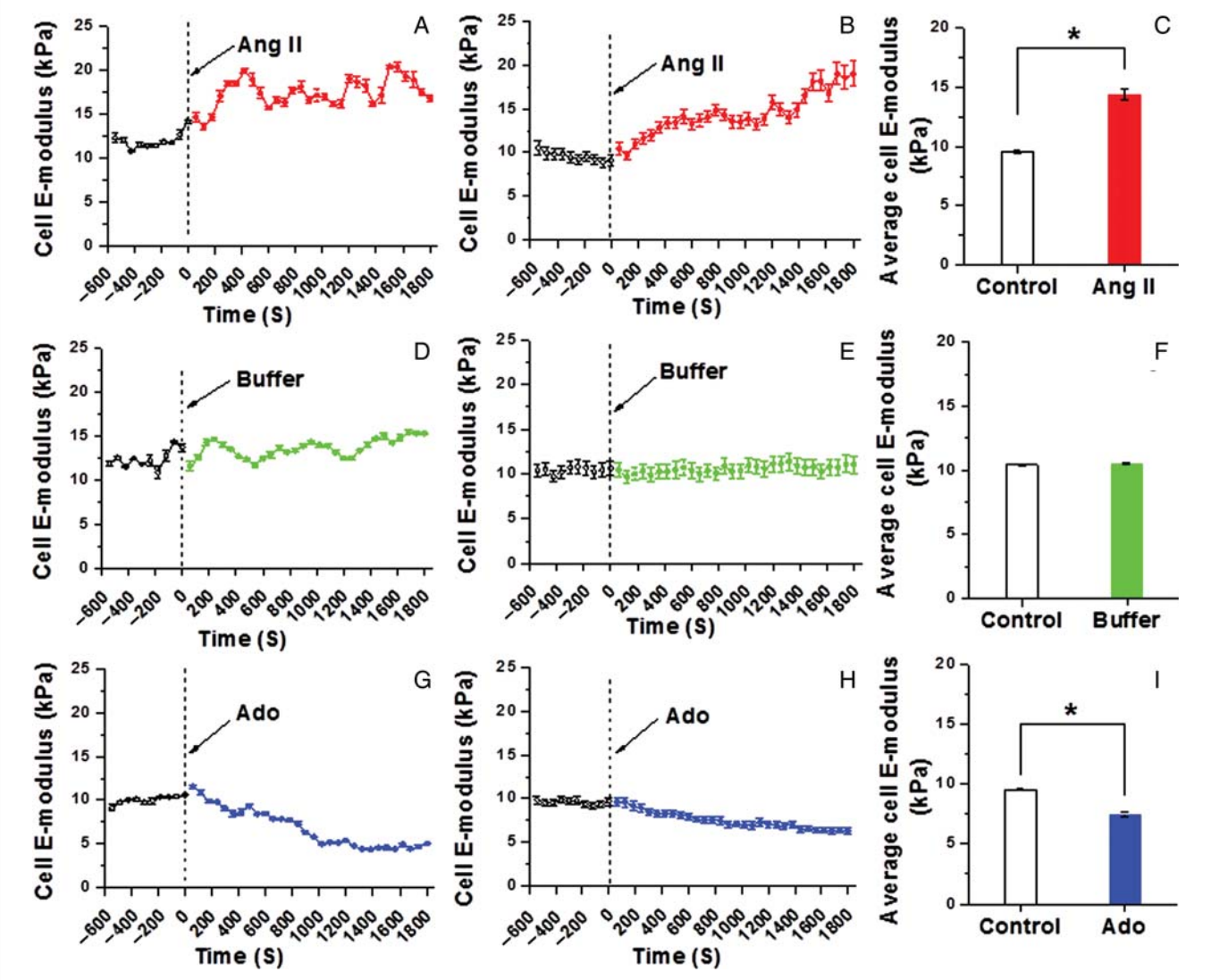

Figure 1 Continuous real-time VSMC stiffness recordings following Ang II or Ado. (*A*) Representative single cell record of VSMC elastic modulus before and after addition of Ang II (10^{-6} M). (*B*) Group average of VSMC elastic modulus alteration before and after addition of Ang II ($n = 10$). (*C*) Average elastic modulus summed across all time points for the group of VSMCs before and after the addition of Ang II ($n = 10$, $^*P < 0.05$). (*D*) Representative single-cell measurement of elastic modulus before and after the addition of cell buffer only. (*E*) Group average of VSMC elastic modulus alteration after treatment with buffer vehicle only ($n = 10$). (*F*) Average elastic modulus summed for all time points of VSMC before and after treatment with buffer ($n = 10$). (*G*) Representative alteration in VSMC elastic modulus before and after the addition of Ado (10^{-4} M). (*H*) Group average of VSMC elastic modulus alteration before and after the addition of Ado ($n = 8$). (*I*) Average elastic modulus summed for all time points of VSMC before and after addition of Ado ($n = 8$, $^*P < 0.05$). Data were acquired at 0.1 Hz of indentation frequency and are presented as mean ± SEM.

the deflection of the cantilever. *E*-modulus is calculated by the transformation of Eqs. (1) to (2).

$$E = \frac{3(1-\nu^2)}{4\sqrt{r_b}} \cdot \frac{F}{\delta^{3/2}}.$$

Unbinding force of FN/$\alpha_5\beta_1$ adhesion complex was determined as the product of the rupture height and cantilever spring constant.

In this study, the location of each unbinding event along the retraction curve relative to the estimated contact point in associated approaching curve was defined as the rupture length. This represents the distance through which the AFM was retracted from the cell membrane before a rupture event was recorded (Supplementary material online, *Figure S4*).

2.5 Statistical analysis

Data are reported as the average ± SEM. Statistically significant differences between the elasticity or adhesion events per curve for comparisons of pre-drug controls and post-drug treatments were analysed with one-way ANOVA, since these data were normally distrusted. Statistically significant differences between the average adhesion force of control and post-drug stimulation were calculated using the Wilcoxon signed-rank test due to the non-normal distribution of these data. A value of $P < 0.05$ was considered significant.

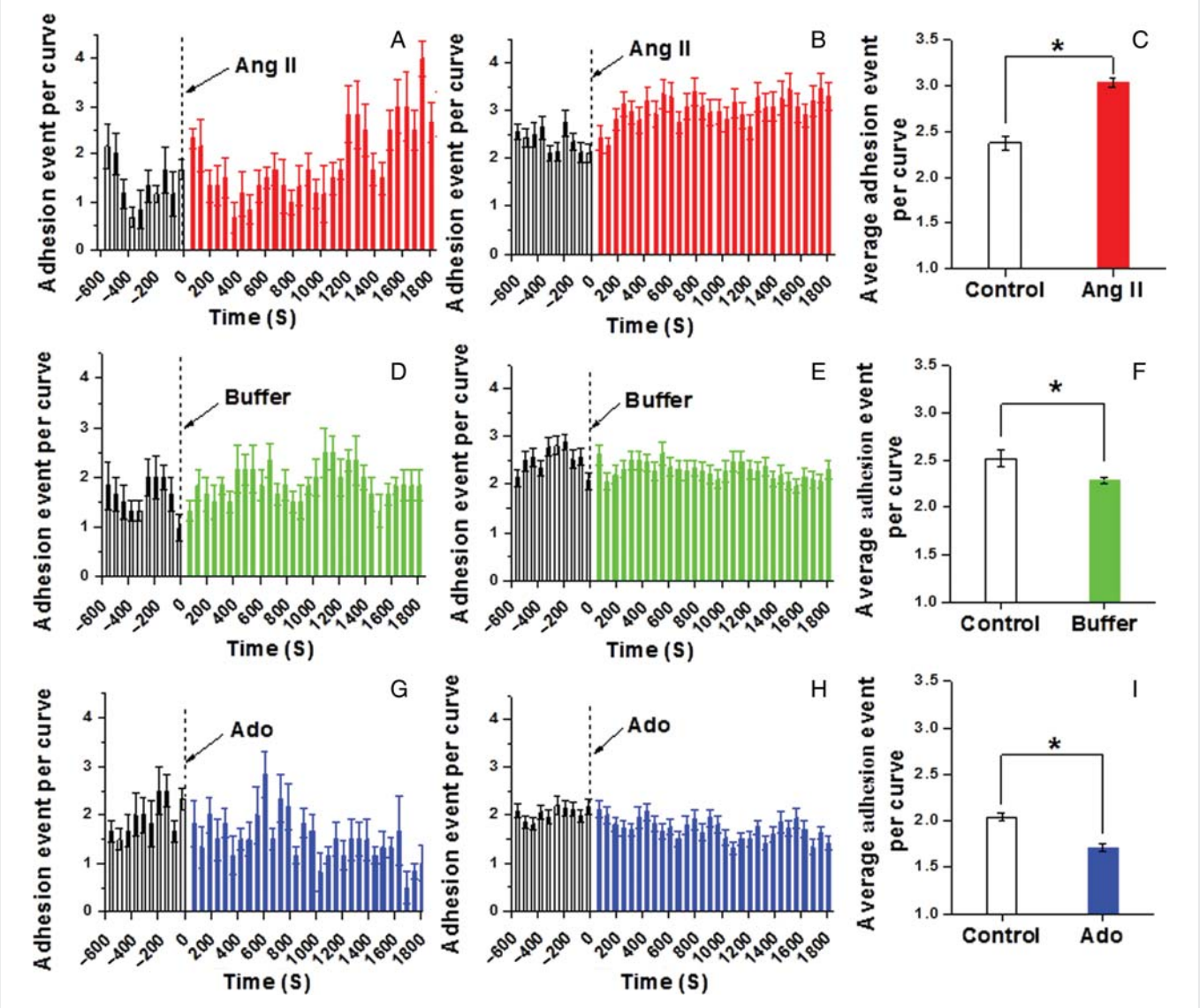

Figure 2 Continuous real-time recordings of adhesion events between VSMCs and FN-coated AFM probe following Ang II or Ado. (*A*) Representative alteration in the number of adhesion events per AFM retraction curve before and after stimulation with Ang II. (*B*) The alteration of group average number of adhesion event per retraction curve before and after the addition of Ang II ($n = 10$). (*C*) Average number of adhesion events per retraction curve before and after addition of Ang II summed over 1800 s ($n = 10$, $^*P < 0.05$). (*D*) Representative change in the number of adhesion event per AFM retraction curve before and after the administration of buffer in cell bath. (*E*) The alteration of group average number of adhesion event per retraction curve before and after the addition of buffer ($n = 10$). (*F*) The average number of adhesion event per retraction curve before and after the addition of buffer summed over 1800 s ($n = 10$, $^*P < 0.05$). (*G*) Representative alteration in the number of adhesion event per AFM retraction curve before and after stimulation with Ado. (*H*) The alteration of group average number of adhesion event per retraction curve before and after the addition of Ado ($n = 8$). (*I*) The average number of adhesion event per retraction curve before and after the addition of Ado summed over 1800s ($n = 8$, $^*P < 0.05$). Data were acquired at 0.1 Hz of indentation frequency and are presented as mean $\pm$ SEM.

3. Results

3.1 VSMC elasticity/stiffness increases with a vasoconstrictor agonist and decreases with a vasorelaxant agonist

Representative tracing of increase in VSMC cortical stiffness (Young's modulus of elasticity; E-modulus) in response to the vasoconstrictor angiotensin II (Ang II) (10^{-6} M) is shown in *Figure 1A*. During a 10 min pre-drug control measurement period, the cell E-modulus was ~12 kPa. For this cell, treatment with Ang II resulted in an increase in E-modulus over the 1800 s period of observation to ~17 kPa. *Figure 1B* shows the group mean increase (~70%) in cell stiffness for 10 independent experiments following the addition of Ang II. The averaged elastic modulus summed over all time points was significantly increased by stimulation with Ang II (*Figure 1C*, $n = 10$, $^*P < 0.05$). Experiments with buffer alone were used as sham control experiments. No significant change occurred in cell stiffness following the addition of buffer-only to the cell bath [*Figure 1D, E* ($n = 10$), and *F* ($n = 10$)]. Upon treatment with the vasorelaxant

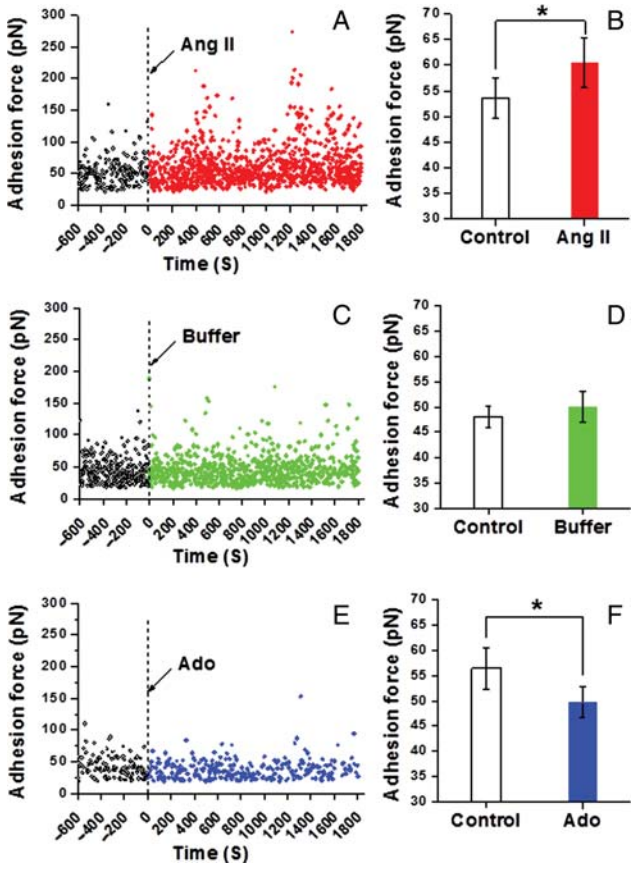

Figure 3 Adhesion rupture forces between VSMCs and FN following Ang II or Ado. (*A*) Representative real-time recording of the force required to rupture an adhesion between FN and VSMCs on a single VSMCs before and after Ang II treatment. (*B*) Average adhesion force between FN and VSMCs before and after Ang II stimulation summed over 1800s ($n = 10$, $^*P < 0.05$). (*C*) Representative real-time record of the adhesion between FN and VSMCs on single VSMCs before and after the administration of buffer in cell bath. (*D*) Average adhesion force between FN and VSMCs before and after the addition of buffer in cell bath summed over 1800 s ($n = 10$). (*E*) Representative real-time record of the adhesion force between FN and VSMCs on single VSMCs before and after Ado treatment. (*F*) Average adhesion force between FN and VSMCs before and after Ado stimulation summed over 1800 s ($n = 8$, $^*P < 0.05$). Data were acquired at 0.1 Hz of indentation frequency. Data for bar graphs are presented as mean ± SEM.

Ado (10^{-4} M), VSMC stiffness decreased (~30%). *Figure 1G* shows a representative single cell trace and *Figure 1H* shows the group mean ($n = 8$ cells). Average elastic modulus summed for all time points showed a significant decrease upon the addition of Ado to cell bath (*Figure 1I*, $n = 8$, $^*P < 0.05$).

3.2 Adhesion to FN is enhanced by a vasoconstrictor and reduced by a vasorelaxant

Changes in integrin adhesion were assessed by the quantification of adhesion events in AFM retraction curves and adhesion rupture force. *Figure 2A* (single cell), *Figure 2B* (group; $n = 10$), and *Figure 2C* (1800 s time sum; $n = 10$) show that stimulation with the vasoconstrictor Ang II led to a significant increase (~27%) in the number of recorded adhesion events between the cell and FN-coated AFM probe. In comparison, the vasorelaxant Ado decreased adhesion (~15%) to FN as shown in *Figure 2G* (single cell), *Figure 2H* (group; $n = 8$), and *Figure 2I* (1800 s time sum; $n = 8$). In control experiments with buffer alone, a small decrease in the number of adhesions per curve (~9%) was observed [*Figure 2D* (single cell), *Figure 2E* (group; $n = 10$), and *Figure 2F* (1800 s time sum; $n = 10$)]. The recordings of adhesion force for representative cells (*Figure 3A, C*, and *E*) and group data (*Figure 3B, D*, and *F*) also show that Ang II significantly increased the adhesion rupture forces indicating tighter bonding between the FN-coated AFM probe and the VSMCs. Buffer alone caused no change in adhesion rupture forces and Ado significantly decreased adhesion rupture forces.

3.3 Analysis of pulling distance before adhesion rupture indicates increased cytoskeletal anchorage of integrin adhesion after a vasoconstrictor and decreased anchorage after a vasorelaxant

Figure 4A shows the frequency distribution of probe retraction distances at which adhesion rupture occurred and demonstrates that most ruptures occur at distances of ≤400 nm. *Figure 4B* shows that at retraction lengths <400 nm that higher adhesion rupture forces were recorded than at longer pulling distance beyond 400 nm. This

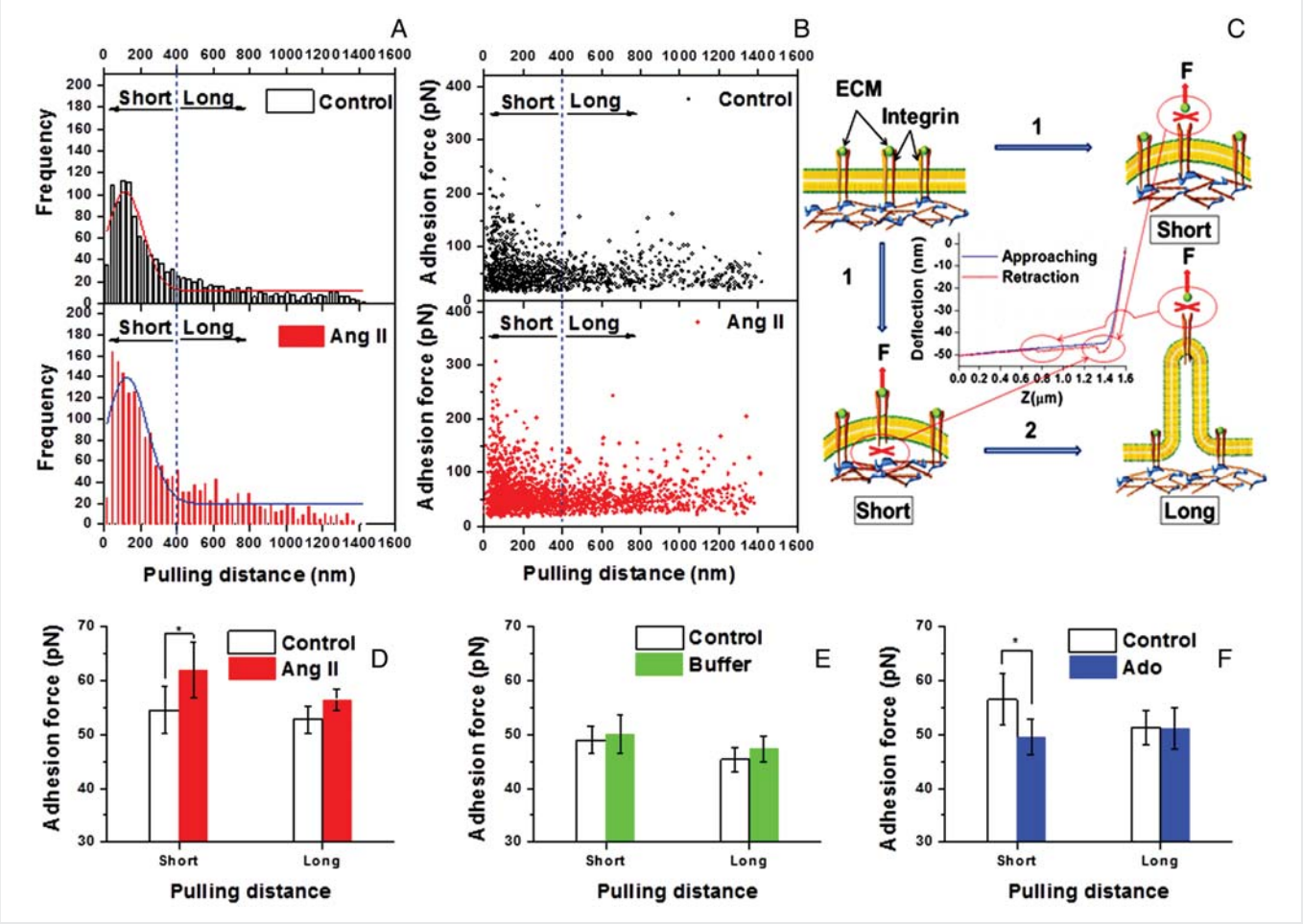

Figure 4 Analyses of relationship between retraction distances and occurrence adhesion rupture. (*A*) Distribution of retraction distances at the time of adhesion rupture. (group/$n = 10$, only the last 600 s post-Ang II treatment data were included for comparison with the 600 s control recording to normalize for the recording time period). (*B*) The adhesion rupture force vs. retraction distance at the time of rupture (group/$n = 10$, only the last 600 s post-Ang II treatment data were included to normalize for the recording time period). (*C*) Illustration of possible adhesion models. (1) During short retraction from the cell the recorded rupture force is higher because of stronger attachment within the FN–integrin–cytoskeletal complex; (2) When the pulling force exerted on the cell exceeds the adhesion rupture force necessary to break connections within the FN–integrin–cytoskeletal complex the cell membrane is believed to deform into a lipid nanotube resulting in a second population of lower rupture force adhesion that break at and longer distances. The deflection signal (nm) of force curve was transformed to force signal (pN) by multiplying with the spring constant of the AFM cantilever. (*D*) Average adhesion rupture force between FN and VSMCs at long- ($\leq$400 nm) and short- (>400 nm) pulling distance before and after Ang II stimulation ($n = 10$, $^*P < 0.05$). (*E*) Average adhesion rupture force between FN and VSMCs at long- and short-pulling distance before and after the addition of buffer in cell bath ($n = 10$). (*F*) Average adhesion rupture force between FN and VSMCs at long- and short-pulling distance before and after Ado stimulation ($n = 8$, $^*P < 0.05$). Data were acquired at 0.1 Hz of indentation frequency. Data for bar graphs are presented as mean $\pm$ SEM.

relationship is indicative of two populations of adhesions with different rupture behaviours, one rupturing with high force and short-pull lengths and the second rupturing with lower forces and long-pull lengths (*Figure 4B*). High force-short-pull adhesions have been interpreted to be associated with receptors that are anchored to the cell cytoskeleton, whereas low force-long-pull adhesions are interpreted to be associated with membrane tethers that are pulled from the membrane as the receptor connections with the cytoskeleton are weak (*Figure 4C*).[33] In our study, Ang II and Ado most strongly affect the high force-short-pull length adhesion population (*Figure 4D–F*).

4. Discussion

Our results demonstrate that the regulation of ECM adhesion and the contractile activation state of vascular smooth muscle are dynamically linked. We tested the hypothesis that the contractile activation of VSMCs with a vasoconstrictor would enhance adhesion to ECM and that the change in adhesive behaviour would be coordinated with a detectable increase in VSMC cortical stiffness as an indication of a change in contractile activation. Likewise, we postulated that treatment with a vasorelaxant would produce the opposite changes and be characterized by reduced ECM adhesion and a parallel

reduction in VSMC cortical stiffness. Real-time measurements of cell stiffness and adhesion with an AFM directly confirmed an immediate increase in VSMC stiffness upon stimulation with Ang II that was paralleled by a significant increase in cellular adhesion to FN and a decrease in stiffness paralleled by a reduction in adhesion following Ado treatment.

The changes in VSMC stiffness are consistent with contractile activation-dependent alterations in the cytoskeleton. A change in cell stiffness would be produced by both contractile filament events and/or changes in actin polymerization. In this regard, the protocol used to measure VSMC stiffness resulted in cell surface indentation by the AFM probe of ~100–300 nm. Thus, the changes in stiffness can be viewed as largely representing the cortical stiffness of the cell. That cortical cell stiffness is altered is consistent with previous reports that VSMC contraction and cortical stiffening are parallel cellular processes simultaneously triggered during smooth muscle activation and involving two actin cytoskeletal compartments both contractile and non-contractile.[34–36] The present study strongly supports evidence that cortical cytoskeletal changes occur the following agonist stimulation of VSMCs. Our observation significantly extend previously available data by demonstrating that the cortical stiffness of VSMC can be modulated bi-directionally depending upon stimulation by a vasoconstrictor or a vasodilator agent and that these events are coupled with simultaneous and parallel changes in integrin adhesion.

In previous studies, we have shown that adhesion events and corresponding rupture forces measured with FN-decorated AFM probes are the result of interactions between FN and $\alpha_5\beta_1$ integrin.[7,37] Thus, the increase in adhesion to FN following treatment of VSMCs with Ang II and a decrease in response to the administration of Ado is likely $\alpha_5\beta_1$ integrin dependent. The underlying mechanisms that account for this change in adhesion could reflect mechanical wrinkling or ruffling of the cell membrane induced by the contractile changes in the cell. If this is occurring then it is possible that integrin density per unit area could change and impact the number of detected adhesions. However, it would not affect the strength of the individual adhesion events that was also observed in this study. A more likely alternative mechanism is that the enhanced adhesion following Ang II or weaken by Ado treatment (*Figure 3B* and *F*) is the result of a receptor-dependent inside-out signalling system that is modulating the availability of active integrins on the cell surface. This could occur through direct integrin activation and/or changes in cell surface integrin expression. A change in the coupling of integrins with underlying focal adhesion protein that directly couple to the integrin to the cytoskeleton[38–40] also appears to play a significant role as indicated by the selective alterations in the high force short-pull population of adhesions (*Figure 4C*). During short-AFM probe retraction distances from the cell membrane, the recorded rupture force is thought to be higher because of stronger attachment within the FN–integrin–cytoskeletal complex [*Figure 4C* (1)]. However, when the pulling force exerted on the cell exceeds the adhesion rupture force necessary to break connections within the FN–integrin–cytoskeletal complex, the cell membrane is believed to deform into a lipid nanotube resulting in a second population of lower rupture force adhesions that break at and longer retraction distances [*Figure 4C* (2)].[41,42] Thus, the observed selective effect of Ang II and Ado on the high force short-pull population of adhesions is interpreted to reflect an effect of these agents on protein–protein associations within the FN–integrin–cytoskeletal complex and it is consistent with previous reports that focal adhesion sites are strengthened following smooth muscle cell activation.[43] Our data provide a unique biomechanical verification that supports the occurrence of adaptive changes in adhesion.

In summary, our results definitively show that a potent vasoconstrictor, Ang II, causes rapid increases in adhesion of VSMCs to the ECM that correlates with the contractile activation of the cell as evidenced by increases in cell stiffness. The demonstration that integrin adhesion changes with VSMC contractile state provides an important piece of information further confirming the view that the contraction of VSMCs is accompanied by tighter coupling and relaxation by looser coupling of cells to the ECM. These changes may be important for improving the efficiency and ability of the VSMCs to appropriately adapt itself changes in intracellular and extracellular mechanical forces that would be associated with the transmission of force between the cytoskeleton and the ECM or between the ECM and the cytoskeleton. Likewise dynamic changes in adhesion at sites of ECM attachment could play an important role as part of the process that leads to vascular stiffening that is a significant feature of cardiovascular disease.[23] Application of this new information to our understanding of resistance artery function enhances our existing framework of the knowledge of vasoregulation and the VSMC contractile process. Additional studies will be required to clarify the molecular mechanisms that dynamically link cell contraction and adhesion. This offers the possibility of designing a new category of therapeutic agents to modulate blood vessel function.

Supplementary material

Supplementary material is available at *Cardiovascular Research* online.

Conflict of interest: none declared.

Funding

This work was supported, in part, by 1P01HL095486 and AHA 0835676N.

References

1. Ingber DE. Mechanical signaling and the cellular response to extracellular matrix in angiogenesis and cardiovascular physiology. *Circ Res* 2002;**91**:877–887.
2. Gunst SJ, Zhang W. Actin cytoskeletal dynamics in smooth muscle: a new paradigm for the regulation of smooth muscle contraction. *Am J Physiol Cell Physiol* 2008;**295**: C576–C587.
3. Balasubramanian L, Ahmed A, Lo CM, Sham JS, Yip KP. Integrin-mediated mechanotransduction in renal vascular smooth muscle cells: activation of calcium sparks. *Am J Physiol Regul Integr Comp Physiol* 2007;**293**:R1586–R1594.
4. Delon I, Brown NH. Integrins and the actin cytoskeleton. *Curr Opin Cell Biol* 2007;**19**: 43–50.
5. Goldschmidt ME, McLeod KJ, Taylor WR. Integrin-mediated mechanotransduction in vascular smooth muscle cells: frequency and force response characteristics. *Circ Res* 2001;**88**:674–680.
6. Schwartz MA, Ginsberg MH. Networks and crosstalk: integrin signalling spreads. *Nat Cell Biol* 2002;**4**:E65–E68.
7. Sun Z, Martinez-Lemus LA, Trache A, Trzeciakowski JP, Davis GE, Pohl U *et al*. Mechanical properties of the interaction between fibronectin and alpha5beta1-integrin on vascular smooth muscle cells studied using atomic force microscopy. *Am J Physiol Heart Circ Physiol* 2005;**289**:H2526–H2535.
8. Martinez-Lemus LA, Wu X, Wilson E, Hill MA, Davis GE, Davis MJ *et al*. Integrins as unique receptors for vascular control. *J Vasc Res* 2003;**40**:211–233.
9. Martinez-Lemus LA, Crow T, Davis MJ, Meininger GA. alphavbeta3- and alpha5beta1-integrin blockade inhibits myogenic constriction of skeletal muscle resistance arterioles. *Am J Physiol Heart Circ Physiol* 2005;**289**:H322–H329.
10. Deng L, Fairbank NJ, Fabry B, Smith PG, Maksym GN. Localized mechanical stress induces time-dependent actin cytoskeletal remodeling and stiffening in cultured airway smooth muscle cells. *Am J Physiol Cell Physiol* 2004;**287**:C440–C448.
11. Zhang W, Gunst SJ. Interactions of airway smooth muscle cells with their tissue matrix: implications for contraction. *Proc Am Thorac Soc* 2008;**5**:32–39.

12. Pelling AE, Li Y, Shi W, Gimzewski JK. Nanoscale visualization and characterization of *Myxococcus xanthus* cells with atomic force microscopy. *Proc Natl Acad Sci U S A* 2005; **102**:6484–6489.
13. Alsteens D, Garcia MC, Lipke PN, Dufrene YF. Force-induced formation and propagation of adhesion nanodomains in living fungal cells. *Proc Natl Acad Sci U S A* 2010; **107**:20744–20749.
14. Stroh C, Wang H, Bash R, Ashcroft B, Nelson J, Gruber H *et al*. Single-molecule recognition imaging microscopy. *Proc Natl Acad Sci U S A* 2004;**101**:12503–12507.
15. Sun Z, Meininger GA. Atomic force microscope-enabled studies of integrin-extracellular matrix interactions in vascular smooth muscle and endothelial cells. *Methods Mol Biol* 2011;**736**:411–424.
16. Rief M, Gautel M, Oesterhelt F, Fernandez JM, Gaub HE. Reversible unfolding of individual titin immunoglobulin domains by AFM. *Science* 1997;**276**:1109–1112.
17. Oberhauser AF, Marszalek PE, Erickson HP, Fernandez JM. The molecular elasticity of the extracellular matrix protein tenascin. *Nature* 1998;**393**:181–185.
18. Baumgartner W, Hinterdorfer P, Ness W, Raab A, Vestweber D, Schindler H *et al*. Cadherin interaction probed by atomic force microscopy. *Proc Natl Acad Sci U S A* 2000;**97**:4005–4010.
19. Sivasankar S, Brieher W, Lavrik N, Gumbiner B, Leckband D. Direct molecular force measurements of multiple adhesive interactions between cadherin ectodomains. *Proc Natl Acad Sci U S A* 1999;**96**:11820–11824.
20. Zhang Y, Sivasankar S, Nelson WJ, Chu S. Resolving cadherin interactions and binding cooperativity at the single-molecule level. *Proc Natl Acad Sci U S A* 2009;**106**:109–114.
21. Sun Z, Martinez-Lemus LA, Hill MA, Meininger GA. Extracellular matrix-specific focal adhesions in vascular smooth muscle produce mechanically active adhesion sites. *Am J Physiol Cell Physiol* 2008;**295**:C268–C278.
22. Lehenkari PP, Horton MA. Single integrin molecule adhesion forces in intact cells measured by atomic force microscopy. *Biochem Biophys Res Commun* 1999;**259**: 645–650.
23. Qiu H, Zhu Y, Sun Z, Trzeciakowski JP, Gansner M, Depre C *et al*. Short communication: vascular smooth muscle cell stiffness as a mechanism for increased aortic stiffness with aging. *Circ Res* 2010;**107**:615–619.
24. Pesen D, Hoh JH. Micromechanical architecture of the endothelial cell cortex. *Biophys J* 2005;**88**:670–679.
25. Carl P, Schillers H. Elasticity measurement of living cells with an atomic force microscope: data acquisition and processing. *Pflugers Arch* 2008;**457**:551–559.
26. Harris AR, Charras GT. Experimental validation of atomic force microscopy-based cell elasticity measurements. *Nanotechnology* 2011;**22**:345102.
27. Schillers H, Walte M, Urbanova K, Oberleithner H. Real-time monitoring of cell elasticity reveals oscillating myosin activity. *Biophys J* 2010;**99**:3639–3646.
28. Kuznetsova TG, Starodubtseva MN, Yegorenkov NI, Chizhik SA, Zhdanov RI. Atomic force microscopy probing of cell elasticity. *Micron* 2007;**38**:824–833.
29. Mathur AB, Collinsworth AM, Reichert WM, Kraus WE, Truskey GA. Endothelial, cardiac muscle and skeletal muscle exhibit different viscous and elastic properties as determined by atomic force microscopy. *J Biomech* 2001;**34**:1545–1553.
30. Lu YB, Franze K, Seifert G, Steinhauser C, Kirchhoff F, Wolburg H *et al*. Viscoelastic properties of individual glial cells and neurons in the CNS. *Proc Natl Acad Sci U S A* 2006;**103**:17759–17764.
31. Costa KD. Single-cell elastography: probing for disease with the atomic force microscope. *Dis Markers* 2003;**19**:139–154.
32. Li QS, Lee GY, Ong CN, Lim CT. AFM indentation study of breast cancer cells. *Biochem Biophys Res Commun* 2008;**374**:609–613.
33. Helenius J, Heisenberg CP, Gaub HE, Muller DJ. Single-cell force spectroscopy. *J Cell Sci* 2008;**121**:1785–1791.
34. An SS, Laudadio RE, Lai J, Rogers RA, Fredberg JJ. Stiffness changes in cultured airway smooth muscle cells. *Am J Physiol Cell Physiol* 2002;**283**:C792–C801.
35. Smith BA, Tolloczko B, Martin JG, Grutter P. Probing the viscoelastic behavior of cultured airway smooth muscle cells with atomic force microscopy: stiffening induced by contractile agonist. *Biophys J* 2005;**88**:2994–3007.
36. Kim HR, Gallant C, Leavis PC, Gunst SJ, Morgan KG. Cytoskeletal remodeling in differentiated vascular smooth muscle is actin isoform dependent and stimulus dependent. *Am J Physiol Cell Physiol* 2008;**295**:C768–C778.
37. Trache A, Trzeciakowski JP, Gardiner L, Sun Z, Muthuchamy M, Guo M *et al*. Histamine effects on endothelial cell fibronectin interaction studied by atomic force microscopy. *Biophys J* 2005;**89**:2888–2898.
38. Choi CK, Vicente-Manzanares M, Zareno J, Whitmore LA, Mogilner A, Horwitz AR. Actin and alpha-actinin orchestrate the assembly and maturation of nascent adhesions in a myosin II motor-independent manner. *Nat Cell Biol* 2008;**10**:1039–1050.
39. Kucik DF, O'Toole TE, Zheleznyak A, Busettini DK, Brown EJ. Activation-enhanced alpha(IIb)beta(3)-integrin-cytoskeleton interactions outside of focal contacts require the alpha-subunit. *Mol Biol Cell* 2001;**12**:1509–1518.
40. Min J, Reznichenko M, Poythress RH, Gallant CM, Vetterkind S, Li Y *et al*. Src modulates contractile vascular smooth muscle function via regulation of focal adhesions. *J Cell Physiol* 2012;**227**:3585–3592.
41. Evans EA, Calderwood DA. Forces and bond dynamics in cell adhesion. *Science* 2007; **316**:1148–1153.
42. Muller DJ, Helenius J, Alsteens D, Dufrene YF. Force probing surfaces of living cells to molecular resolution. *Nat Chem Biol* 2009;**5**:383–390.
43. Turner CE, Pietras KM, Taylor DS, Molloy CJ. Angiotensin II stimulation of rapid paxillin tyrosine phosphorylation correlates with the formation of focal adhesions in rat aortic smooth muscle cells. *J Cell Sci* 1995;**108**(Pt 1):333–342.